ACS OMEGA

http://pubs.acs.org/journal/acsodf

Article

Stabilization of an ^{211}At-Labeled Antibody with Sodium Ascorbate

Shino Manabe,* Hiroki Takashima, Kazunobu Ohnuki, Yoshikatsu Koga, Ryo Tsumura, Nozomi Iwata, Yang Wang, Takuya Yokokita, Yukiko Komori, Sachiko Usuda, Daiki Mori, Hiromitsu Haba, Hirofumi Fujii, Masahiro Yasunaga, and Yasuhiro Matsumura*

Cite This: *ACS Omega* 2021, 6, 14887−14895

Read Online

ABSTRACT: ^{211}At, an α-particle emitter, has recently attracted attention for radioimmunotherapy of intractable cancers. However, our sodium dodecyl sulfate polyacrylamide gel electrophoresis and flow cytometry analyses revealed that ^{211}At-labeled immunoconjugates are easily disrupted. Luminol assay revealed that reactive oxygen species generated from radiolysis of water caused the disruption of ^{211}At-labeled immunoconjugates. To retain their functions, we explored methods to protect ^{211}At-immunoconjugates from oxidation and enhance their stability. Among several other reducing agents, sodium ascorbate most safely and successfully protected ^{211}At-labeled trastuzumab from oxidative stress and retained the stability of the ^{211}At-labeled antibody and its cytotoxicity against antigen-expressing cells for several days.

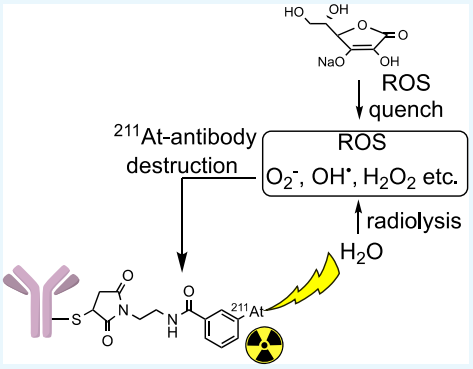

INTRODUCTION

Radioimmunotherapy (RIT) is defined as targeted radionuclide therapy using radiolabeled antibodies. RIT has expanded the applications of radiotherapy from focusing on local tumors to targeting scattered tumors, such as distant metastases and disseminated lesions. As for β-particles, two kinds of radiopharmaceuticals, which target the CD20 molecule on the surface of lymphoma cells, ^{90}Y-labeled rituximab and ^{131}I-labeled rituximab, have already shown clinical benefits against CD20-positive non-Hodgkin B-cell lymphoma.[1] Compared with β-particles, α-particles have more potent linear energy transfer (LET) and a shorter path range. Owing to their high-energy emission within a short path length, α-particles can selectively eliminate target cells with minimal radiation damage to the surrounding normal tissues when delivered selectively to tumor tissues. These properties render α-particles an attractive tool for treating intractable tumors.[2−5] ^{211}At is an α-emitter with a short half-life (7.2 h) and does not yield cytotoxic daughter isotopes during its decay; the first branch (58.2%) decays through electron capture to ^{211}Po (half-life: 516 ms), which decays through α-particle emission to ^{207}Bi (half-life: 31.55 y). The second branch (41.8%) directly decays through α-particle emission to ^{207}Bi. ^{207}Bi results in stable ^{207}Pb via its metastable states after the electron capture. To harness the short path of α-particles and potent LET, ^{211}At must be precisely delivered to the target. For delivering ^{211}At to the desired regions, ^{211}At-labeled small molecules, including uridine analogues,[6] benzylguanidine (a norepinephrine analogue),[7] biotin analogues,[8] a phenylalanine derivative,[9] and bisphosphonate complexes, have been previously designed.[10] Furthermore, ^{211}At-labeled antibodies were reportedly tested to deliver highly cytotoxic ^{211}At to the target in preliminary investigations and preclinical situations.[11−18] The ^{211}At-labeled anti-Tenascin mAb 81C6 was administered locally to 18 patients with recurrent malignant brain tumors,[11] and the ^{211}At-labeled MX35 F(ab′)$_2$, targeting the sodium-dependent phosphate transport protein 2B, was intraperitoneally administered to nine patients with ovarian cancer.[12] In addition to the promising results obtained by these studies, the procedure for the production of ^{211}At-labeled antibodies under the current Good Manufacturing Practices (cGMP) toward clinical application was recently reported.[19] To maximize the functions of ^{211}At-labeled antibodies, the quality of the conjugates must be validated. Therefore, in the present study, we evaluated the quality of an ^{211}At-conjugated antibody. Several reports on the disruption of radioimmunoconjugates by reactive oxygen species (ROS), determined by functional analyses, have been published.[20−24] In this paper, we clearly show the disruption of the ^{211}At-conjugated antibody by ROS generated from water radiolysis through various approaches including sodium dodecyl sulfate−polyacrylamide gel electrophoresis (SDS−PAGE). The ROS concentration was measured using a luminol assay system, and the degradation was

Received: February 5, 2021
Accepted: May 20, 2021
Published: May 31, 2021

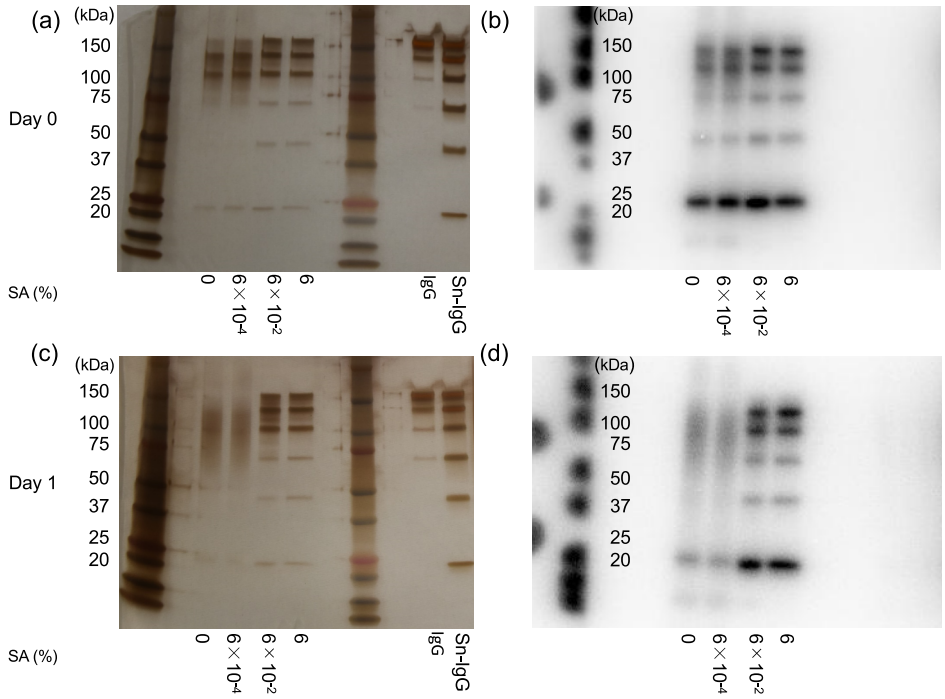

Figure 1. Sodium dodecyl sulfate−polyacrylamide gel (SDS−PAGE) and autoradiography for ^{211}At-labeled trastuzumab. SA concentrations (mg/mL) are indicated. SDS−PAGE and autoradiography were performed to determine the effects of SA on the stability of the immunoconjugate. (a) Polyacrylamide gel on day 0 and (b) autoradiograph of ^{211}At-labeled trastuzumab on day 0 and (c) polyacrylamide gel after 1 d and (d) ^{211}At-labeled trastuzumab after 1 d.

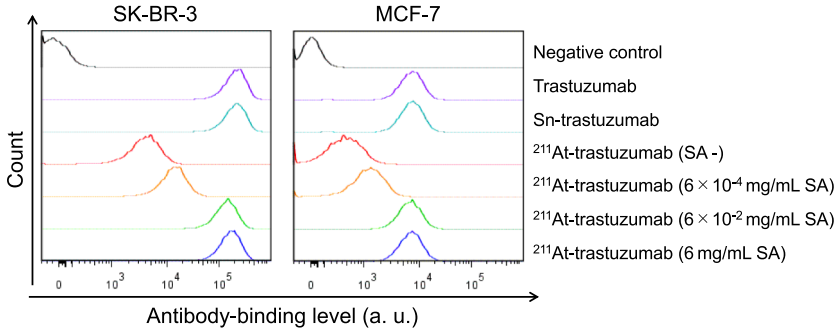

Figure 2. Flow cytometry analysis of the binding activity of ^{211}At-labeled trastuzumab to human epidermal growth factor receptor 2 (HER2)-expressing cells. ^{211}At-labeled trastuzumab with or without SA at the indicated concentrations facilitated binding with breast cancer cell lines having different HER2 expression levels. SK-BR-3: high HER2 expression; MCF-7: low HER2 expression. Sn-trastuzumab is *N*-[2-(maleimido)ethyl]-3-(trimethylstannyl)benzamide-conjugated trastuzumab. Negative control is a sample incubated with only the secondary antibody. The flow cytometry analysis was performed 6 d after ^{211}At labeling.

suppressed by quenching ROS by addition of sodium ascorbate (SA), a safe (or non-cytotoxic) reducing agent.

■ RESULTS AND DISCUSSION

Evaluation of the Effects of SA Concentration on the Stability of ^{211}At-Labeled Trastuzumab by SDS−PAGE, Autoradiography, and Flow Cytometry Assay. ^{211}At-labeled trastuzumab was prepared according to the previously described procedures.[13,25,26] The effects of different concentrations of SA on the stability of ^{211}At-labeled trastuzumab were evaluated using SDS−PAGE, and autoradiography was performed on the day of ^{211}At labeling and on the following day (Figure 1). Even on the day of ^{211}At labeling, ^{211}At-labeled trastuzumab was slightly disrupted in the absence of SA (Figure 1a,b). On the following day, ^{211}At-labeled trastuzumab was completely disrupted in the presence of less than 6×10^{-4} mg/mL SA (Figure 1c,d). These results indicate that the astatinated antibodies were disrupted in a time-dependent manner. In contrast, ^{211}At-labeled trastuzumab in the presence of more than 6×10^{-2} mg/mL SA was still stable on the following day, thus indicating the concentration-dependent protective effects of SA.[27]

The binding activity (binding activity = MI − MI_{NC}) of ^{211}At-labeled trastuzumab to high (SK-BR-3) and low (MCF-7) human epidermal growth factor receptor 2 (HER2)-expressing cell lines was investigated using flow cytometry, where MI is defined as median intensities of samples incubated with trastuzumab, Sn-trastuzumab, or ^{211}At-trastuzumab and MI_{NC} is median intensities of negative control, which is the sample incubated with only the secondary antibody.

Binding activities of trastuzumab, *N*-[2-(maleimido)ethyl]-3-(trimethylstannyl)benzamide-conjugated trastuzumab (Sn-tras-

https://doi.org/10.1021/acsomega.1c00684
ACS Omega 2021, 6, 14887−14895

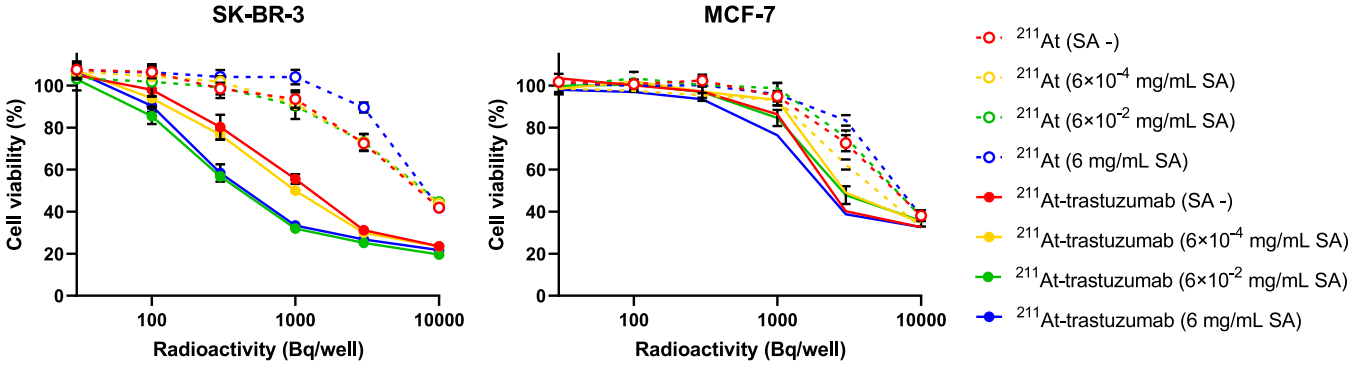

Figure 3. Cytotoxic effects of ^{211}At-labeled trastuzumab in breast cancer cell lines. The cytotoxic effects of ^{211}At-labeled trastuzumab with and without SA on breast cancer cell lines with different expression levels of human epidermal growth factor receptor 2 (HER2) were determined using the WST-8 cell count assay. SK-BR-3: high HER2 expression; MCF-7: low HER2 expression. N = 4. Data are presented as mean ± standard deviation (SD) values.

tuzumab), and astatinated trastuzumab (^{211}At-trastuzumab) in phosphate-buffered saline (PBS) for SK-BR-3 cells were 2.01×10^5, 1.98×10^5, and 3.91×10^3, respectively (Figure 2). Binding activities of ^{211}At-trastuzumab in 6×10^{-4}, 6×10^{-2}, and 6 mg/mL SA to SK-BR-3 cells were 1.29×10^4, 1.33×10^5, and 1.59×10^5, respectively. In the presence of more than 6×10^{-2} mg/mL SA, the binding activity of ^{211}At-trastuzumab was maintained. The binding affinities of trastuzumab and functionalized trastuzumab to MCF-7 cells were weak because of their low HER2 expression levels.

***In Vitro* Cytotoxicity Evaluation of ^{211}At-Labeled Trastuzumab.** The cytotoxicity of ^{211}At-labeled trastuzumab was evaluated using the WST-8 assay. The cytotoxic effects of ^{211}At-labeled trastuzumab on cancer cells depended on HER2 expression levels on the cell surface. Astatinated trastuzumab killed SK-BR-3 cells more efficiently than free ^{211}At. However, the differences in the cytocidal effects on MCF-7 cells between free ^{211}At and the immunoconjugates were minor. Based on the protective effects on the binding activities of ^{211}At-trastuzumab, SA contributed to the cytocidal effects of the immunoconjugates in a dose-dependent manner (Figure 3). ^{211}At-trastuzumab in 6×10^{-2} and 6 mg/mL SA exerted greater cytocidal effects on SK-BR-3 cells than ^{211}At-trastuzumab in PBS and 6×10^{-4} mg/mL SA.

Detection of ROS Using Luminol Assay. We speculated that antibody damage was caused by ROS generated through the interaction of water molecules and α-particles emitted from ^{211}At. ROS can be detected using chemiluminescent luminol assay. The luminol assay can measure the global levels of ROS, such as H_2O_2, O_2^-, and $OH^\bullet$, with high sensitivity under physiological conditions and can be sensitized by the addition of horseradish peroxidase.[28]

Thus, we performed the luminol assay to quantify the ROS in ^{211}At and ^{211}At-conjugated antibody solutions (adjusted to approximately the same radioactivity) with different SA concentrations (Figure 4). On addition of SA at a low concentration (6×10^{-4} mg/mL), the same level of luminol reactivity was detected as in the SA-free sample in both ^{211}At and ^{211}At-labeled trastuzumab. Although low levels of ROS were detected in 6×10^{-2} mg/mL SA ^{211}At solution, the levels were below the detection limit in ^{211}At-labeled antibody solution. The reason for this difference is unclear at this moment. The intensity of chemiluminescence in the samples with 6 mg/mL SA was lower than the detection limit. These results suggest that SA greatly contributes to the reduction in the amount of ROS.

Scope of Reducing Agents. The scope of reducing agents, in addition to SA, potentially applicable for reducing ROS levels was investigated. We used agents with other mechanisms of reduction, namely, L-cysteine, sodium hydrosulfite, and maltose. The reducing ability of L-cysteine and sodium hydrosulfite is because of the redox potential of the sulfur atom, whereas that of maltose is inherent in its hemiacetal structure. The concentrations of these reducing agents were set to 6×10^{-2} mg/mL based on the SA threshold. We performed a luminol assay to assess the ROS-quenching abilities of various reducing agents in solutions of free ^{211}At and ^{211}At-labeled trastuzumab (Figure 5). The order of the reducing abilities of the agents in the ^{211}At-labeled trastuzumab solution was SA > L-cysteine ≥ sodium hydrosulfite > maltose (Figure 5b). We found that 6×10^{-2} mg/mL L-cysteine did not completely quench ROS in the ^{211}At-labeled antibody solution, although it efficiently quenched ROS in the solution of free ^{211}At (Figure 5a). At present, the reason for the difference in ROS concentration in the solutions of free ^{211}At and ^{211}At-labeled antibody in the presence of 6×10^{-2} mg/mL L-cysteine is unclear.

SDS−PAGE revealed that maltose or sodium hydrosulfite could not adequately protect the astatinated antibodies (Figure 6). However, SA and L-cysteine protected the immunoconjugates from oxidative stress. These results are in agreement with the ROS concentration measured by luminol assay.

Accordingly, ^{211}At-labeled trastuzumab solution containing L-cysteine or SA displayed high binding activity to SK-BR-3 and MCF-7 cells (Figure 7), depending on the surface HER2 expression levels, and these results were comparable to those obtained for the naked and linker-attached trastuzumab before astatination. However, compared with the ^{211}At-labeled trastuzumab protected with SA or L-cysteine, the astatinated antibodies with maltose or sodium hydrosulfite did not retain their binding activity. The binding activities of trastuzumab and Sn-trastuzumab to SK-BR-3 cells were 1.50×10^5 and 1.42×10^5, respectively. Binding of ^{211}At-trastuzumab in PBS, ^{211}At-trastuzumab in 6×10^{-2} mg/mL sodium hydrosulfite, and ^{211}At-trastuzumab in 6×10^{-2} mg/mL maltose to SK-BR-3 cells became weak, with activities of 1.84×10^3, 7.77×10^2, and 7.57×10^3, respectively. ^{211}At-trastuzumab in 6×10^{-2} mg/mL SA and ^{211}At-trastuzumab in 6×10^{-2} mg/mL L-cysteine retained binding activities of 6.61×10^4 and 7.77×10^4, respectively. In MCF-7 cells, the binding activities of trastuzumab, Sn-trastuzumab, ^{211}At-trastuzumab in PBS, ^{211}At-trastuzumab in 6×10^{-2} mg/mL SA, ^{211}At-trastuzumab in 6×10^{-2} mg/mL L-cysteine, ^{211}At-trastuzumab in 6×10^{-2} mg/mL sodium

https://doi.org/10.1021/acsomega.1c00684
ACS Omega 2021, 6, 14887−14895

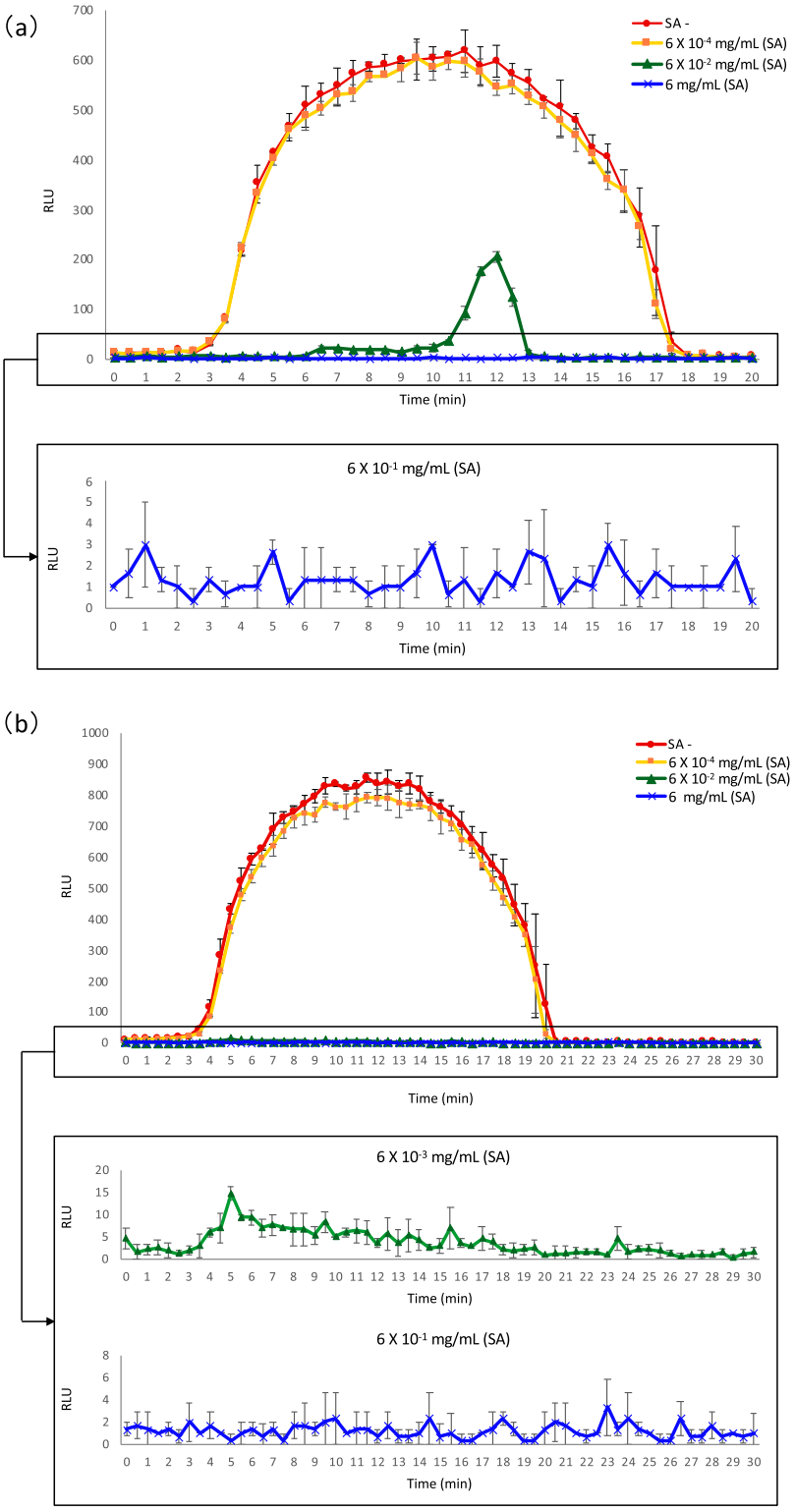

Figure 4. Detection of ROS using luminol assay. (a) SA was added at different concentrations to ^{211}At in PBS. The lower (boxed) graph is an expansion of the 6 mg/mL SA addition protocol. (b) SA was added at different concentrations to ^{211}At-labeled trastuzumab in PBS. The lower (boxed) graphs are expansions of 6×10^{-2} and 6 mg/mL SA addition protocols. RLU = relative luminescence units. Data are presented as mean ± SD values.

hydrosulfite, and ^{211}At-trastuzumab in 6×10^{-2} mg/mL maltose were 8.11×10^3, 7.87×10^3, 2.96×10^2, 6.78×10^3, 7.28×10^3, 1.33×10^2, and 1.08×10^3, respectively. Regarding cytotoxicity, ^{211}At-labeled trastuzumab with L-cysteine had the same potency as ^{211}At-labeled trastuzumab with SA, and the astatinated antibodies with these protectants exerted greater cytotoxic effects than the immunoconjugate without the protectant (Figure 7). However, the astatinated antibodies with maltose or sodium hydrosulfite displayed antitumor activities that were less than or similar to those of the immunoconjugate without the protectant.

https://doi.org/10.1021/acsomega.1c00684
ACS Omega 2021, 6, 14887−14895

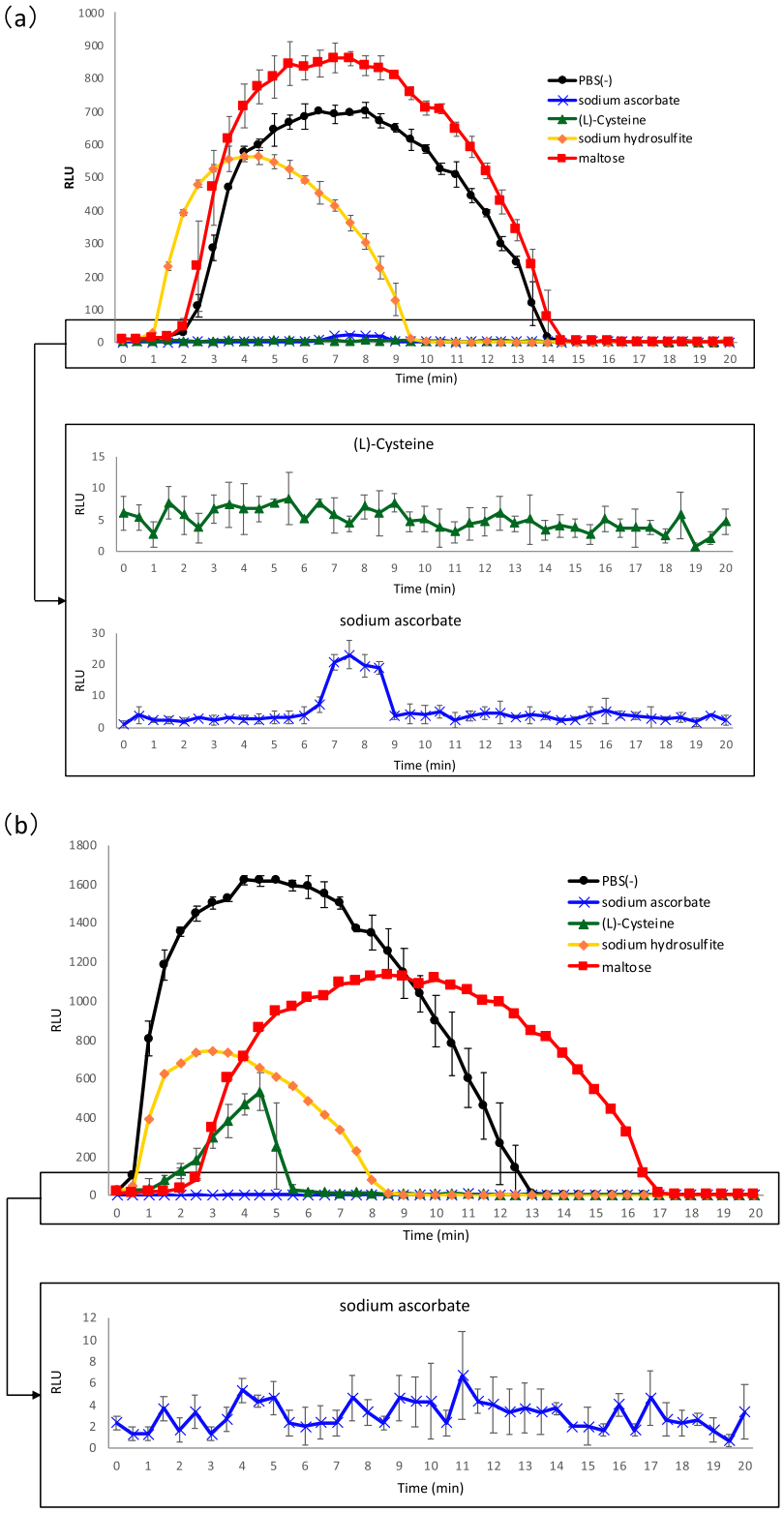

Figure 5. Quenching potential of different reducing agents for ROS in ^{211}At or ^{211}At-labeled trastuzumab solutions, as assessed using the luminol assay. (a) Reducing agents (6×10^{-2} mg/mL) were added to ^{211}At in PBS. (b) Reducing agents (6×10^{-2} mg/mL) were added to ^{211}At-labeled trastuzumab in PBS.

■ CONCLUSIONS

In this study, we longitudinally investigated the quality of conjugates after labeling of antibodies with ^{211}At, a promising α-emitter applicable for targeted alpha therapy. Our results indicate that the radioimmunoconjugates were severely degraded within 1 day of labeling with ^{211}At. Although these devastating effects of α-particle emitters on macromolecules, such as proteins, have been reported previously, the mechanism underlying the destruction of macromolecules including antibodies *in vivo* has not been clarified as of now. Here, we

https://doi.org/10.1021/acsomega.1c00684
ACS Omega 2021, 6, 14887−14895

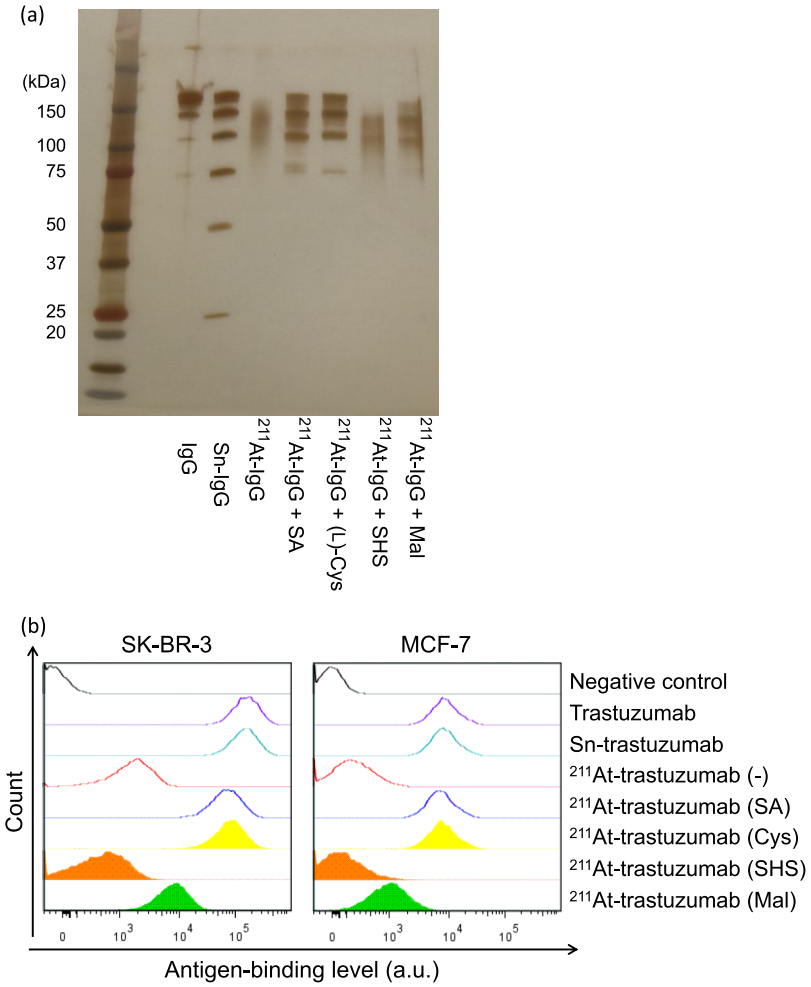

Figure 6. (a) Sodium dodecyl sulfate-polyacrylamide gel electrophoresis (SDS−PAGE) of Sn- and ^{211}At-labeled trastuzumab (IgG) in the presence of various reducing agents. Concentration of each reducing agent is 6×10^{-2} mg/mL. SDS−PAGE analysis was performed 4 d after ^{211}At labeling. (b) Flow cytometry analysis of the binding activity of ^{211}At-labeled trastuzumab to different breast cancer cell lines in the presence of various reducing agents. Cell lines with high (SK-BR-3) and low (MCF-7) human epidermal growth factor receptor 2 (HER2) expression levels were treated with ^{211}At-labeled trastuzumab in the presence of various reducing agents. Flow cytometry analysis was performed 6 d after ^{211}At labeling. SA: sodium ascorbate; Cys: L-cysteine; SHS: sodium hydrosulfite; Mal: maltose. Concentrations of reducing agents are 6×10^{-2} mg/mL. RLU = relative luminescence units.

particularly focused on the high LET of ^{211}At. High-LET particles can strongly induce radiolysis of exposed materials. When the water is irradiated, numerous types of radicals, primarily ROS in water solutions, are produced. In this study, using luminol assay, SDS−PAGE, flow cytometry, and cytotoxicity assays, we clearly show that ^{211}At-labeled trastuzumab was degraded by ROS generated from the radiolysis of water.

The mechanism underlying antibody denaturation upon ^{211}At labeling provides insights into the protection against damage caused by radioactive conjugated antibodies.

Certain reducing agents or radial scavengers can suppress ROS upon ^{211}At conjugation.

Our assays were performed 4−6 days after ^{211}At conjugation, with and without the reducing agents. ^{211}At-conjugated trastuzumab was stable in the presence of SA for several days. SDS−PAGE, flow cytometry, and cytotoxicity assays revealed that the minimum concentration of SA for protection of ^{211}At-labeled trastuzumab is 6×10^{-2} mg/mL. Protected ^{211}At-labeled trastuzumab maintained its binding activity and potent antitumor effects on antigen-expressing cells. Although numerous ^{211}At-labeled antibodies have been reported so far, the stability of ^{211}At-labeled immunoglobulin G has remained largely unclear, except in studies using large quantities of ^{211}At-conjugated samples.[19] Overall, our results clearly indicate that protection from oxidative stress is required for ^{211}At immunoconjugation.

The stability and biodistribution of ^{211}At-labeled antibodies are important considerations for α-particle conjugation; hence, the structure of the conjugated antibody needs to be maintained, as observed upon the addition of SA. In the presence of 6×10^{-2} mg/mL SA, the ^{211}At-labeled antibody was stable for several days.

The selection of reducing agents is important in RIT using ^{211}At-labeled antibodies. In this case, reducing agents should have an efficient ROS-quenching ability and less toxicity. The results of our experiments indicate that SA and L-cysteine are good candidates for use as reducing agents. Because SA is frequently added as a stabilizing agent in clinically approved formulations, SA addition is highly practicable. The toxicity of reducing agents is also important when clinical application is considered. LD_{50} (rat) of SA is 11,900 mg/kg, whereas that of L-cysteine is 1890 mg/kg.[29] Considering that the LD_{50} of SA is

https://doi.org/10.1021/acsomega.1c00684
ACS Omega 2021, 6, 14887−14895

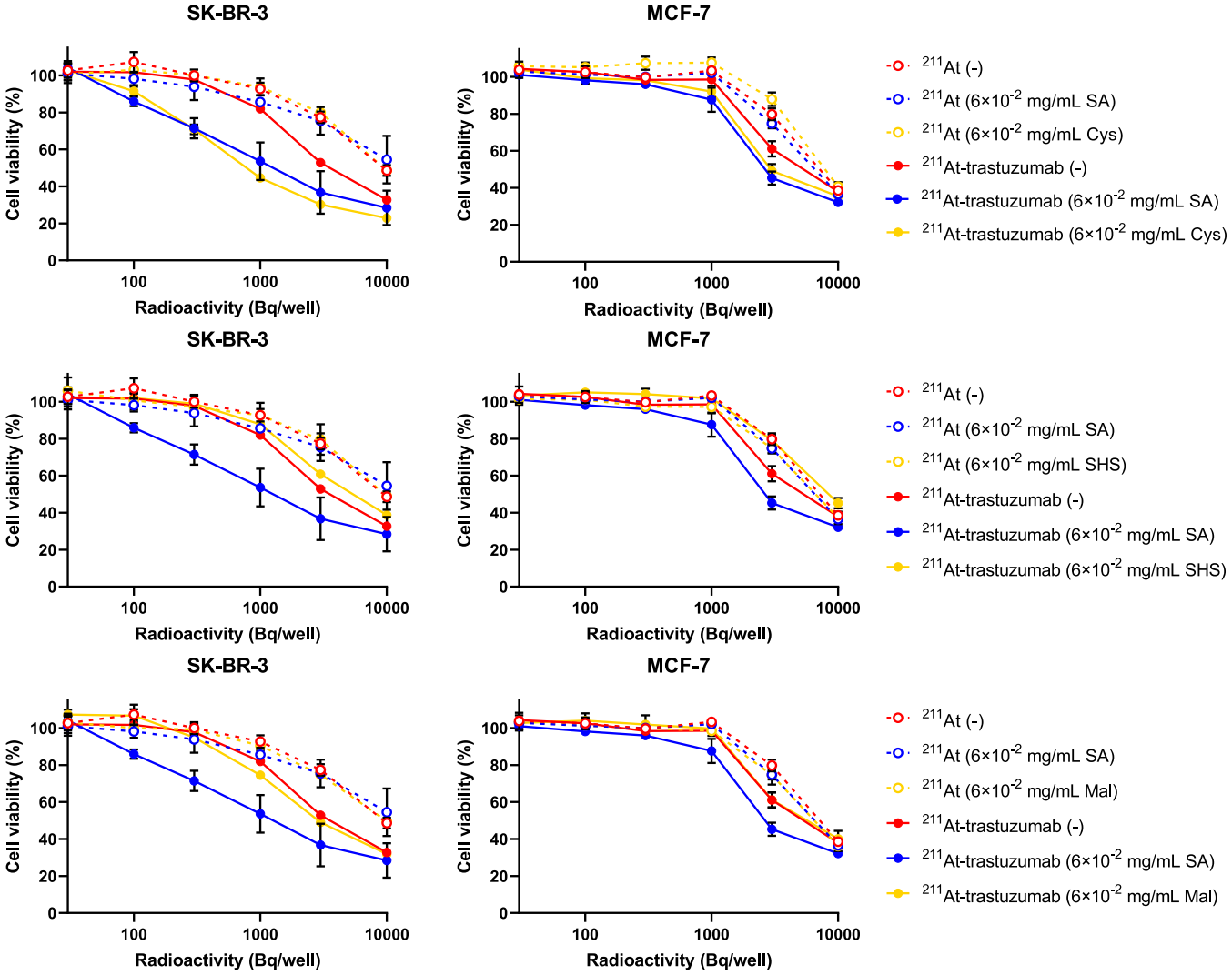

Figure 7. Cytotoxic effects of ^{211}At-labeled trastuzumab in breast cancer cell lines. The cytotoxic effects of ^{211}At-labeled trastuzumab in the presence of reducing agents,SA and L-cysteine, and on breast cancer cell lines with different expression levels of human epidermal growth factor receptor 2 (HER2) were determined using the WST-8 assay. SK-BR-3: high HER2 expression; MCF-7: low HER2 expression. SA: sodium ascorbate; Cys: L-cysteine; SHS: sodium hydrosulfite; Mal: maltose. $N = 4$. Data are presented as mean ± SD values.

extremely high, SA is currently the most effective and safest candidate as a ROS scavenger in the view of toxicity as well.

■ ASSOCIATED CONTENT

Supporting Information

The Supporting Information is available free of charge at https://pubs.acs.org/doi/10.1021/acsomega.1c00684.

General Procedure, ^{211}At generation, preparation of *N*-[2-(maleimido)ethyl]-3-(trimethylstannyl)benzamide-conjugated trastuzumab, ^{211}At labeling of trastuzumab by Sn−^{211}At exchange reaction, detection of ROS using luminol assay, SDS−PAGE, analysis of ^{211}At-labeled antibodies, flow cytometry analysis, *in vitro* cytotoxicity assay, and ^{1}H NMR spectrum of *N*-[2-(maleimido)-ethyl]-3-(trimethylstannyl)benzamide (PDF)

■ AUTHOR INFORMATION

Corresponding Authors

Shino Manabe − *Pharmaceutical Department, Hoshi University, Tokyo 142-8501, Japan; Research Center for Pharmaceutical Development Graduate School of Pharmaceutical Sciences & Faculty of Pharmaceutical Sciences, Tohoku University, Sendai 980-8578, Japan; Glycometabolic Biochemistry Laboratory, RIKEN, Wako, Saitama 351-0198, Japan;* orcid.org/0000-0002-2763-1414; Email: s-manabe@hoshi.ac.jp, shino.manabe.e1@tohoku.ac.jp, smanabe@riken.jp

Yasuhiro Matsumura − *Department of Immune Medicine, National Cancer Center Research Institute, 104-0045 Tokyo, Japan*; Email: yhmatsum@east.ncc.go.jp

Authors

Hiroki Takashima − *Division of Developmental Therapeutics, Exploratory Oncology Research and Clinical Trial Center, National Cancer Center, Kashiwa City 277-8577, Japan*

Kazunobu Ohnuki − *Division of Functional Imaging, Exploratory Oncology Research and Clinical Trial Center, National Cancer Center, Kashiwa City 277-8577, Japan*

Yoshikatsu Koga − *Division of Developmental Therapeutics, Exploratory Oncology Research and Clinical Trial Center and Department of Strategic Programs, Exploratory Oncology*

https://doi.org/10.1021/acsomega.1c00684
ACS Omega 2021, 6, 14887−14895

Research and Clinical Trial Center, National Cancer Center, Kashiwa City 277-8577, Japan
Ryo Tsumura − *Division of Developmental Therapeutics, Exploratory Oncology Research and Clinical Trial Center, National Cancer Center, Kashiwa City 277-8577, Japan*
Nozomi Iwata − *Division of Developmental Therapeutics, Exploratory Oncology Research and Clinical Trial Center, National Cancer Center, Kashiwa City 277-8577, Japan*
Yang Wang − *Nishina Center for Accelerator-Based Science, RIKEN, Wako-shi, Saitama 351-0198, Japan*
Takuya Yokokita − *Nishina Center for Accelerator-Based Science, RIKEN, Wako-shi, Saitama 351-0198, Japan*
Yukiko Komori − *Nishina Center for Accelerator-Based Science, RIKEN, Wako-shi, Saitama 351-0198, Japan*
Sachiko Usuda − *Nishina Center for Accelerator-Based Science, RIKEN, Wako-shi, Saitama 351-0198, Japan*
Daiki Mori − *Nishina Center for Accelerator-Based Science, RIKEN, Wako-shi, Saitama 351-0198, Japan*
Hiromitsu Haba − *Nishina Center for Accelerator-Based Science, RIKEN, Wako-shi, Saitama 351-0198, Japan*
Hirofumi Fujii − *Division of Functional Imaging, Exploratory Oncology Research and Clinical Trial Center, National Cancer Center, Kashiwa City 277-8577, Japan*
Masahiro Yasunaga − *Division of Developmental Therapeutics, Exploratory Oncology Research and Clinical Trial Center, National Cancer Center, Kashiwa City 277-8577, Japan*

Complete contact information is available at:
https://pubs.acs.org/10.1021/acsomega.1c00684

Author Contributions

S.M. and Y.M. conceived and designed the project. Y.K. and R.T. conjugated *N*-[2-(maleimido)ethyl]-3-(trimethylstannyl)-benzamide to trastuzumab. H.T., T.Y., H.H, and S.M. carried out ^{211}At labeling. H.T., K.O., and N.I. performed TLC analysis. K.O. measured ROS by the luminol assay. H.T., K.O., R.T., and N.I. evaluated the astatinated antibodies by SDS−PAGE. H.T. performed flow cytometry. H.T. and Y.K. evaluated cytotoxicity of the astatinated antibodies. T.Y., Y.K., W.Y., D.M., and H.H. prepared ^{211}At and measured radioactivity. H.F., M.Y., and Y.M. supervised the project. S.M., H.T., and K.O. wrote the major part of the paper. All authors analyzed and discussed results and assisted in paper preparation.

Funding

This work was supported by the Project for Cancer Research and Therapeutic Evolution (19cm0106237h0002 to H.T.) from the Japan Agency for Medical Research and Development (AMED), by RIKEN Engineering Network Project (to S.M.), and National Cancer Center Research and Development Fund (29-A-9 to Y.M. and 30-S-4 to Y.K.). The ^{211}At was supplied through the Supply Platform of Short-lived Radioisotopes, supported by the JSPS Grant-in-Aid for Scientific Research on Innovative Areas, grant number 16H06278.

Notes

The authors declare no competing financial interest.

ACKNOWLEDGMENTS

S.M. thanks Professor Hidehiko Nakagawa at the Graduate School of Pharmaceutical Science, Nagoya City University, for intellectual discussions.

ABBREVIATIONS

cGMP, current Good Manufacturing Practices; LET, linear energy transfer; PBS, phosphate-buffered saline; RIT, radioimmunotherapy; ROS, reactive oxygen species; SA, sodium ascorbate; SDS−PAGE, sodium dodecyl sulfate−polyacrylamide gel electrophoresis; SHS, sodium hydrosulfite

REFERENCES

(1) Green, D. J.; Press, O. W. Whither radioimmunotherapy: To be or not to be? *Cancer Res.* **2017**, *77*, 2191−2196.
(2) Aghevlian, S.; Boyle, A. J.; Reilly, R. M. Radioimmunotherapy of cancer with high linear energy transfer (LET) radiation delivered by radionuclides emitting α-particles or Auger electrons. *Adv. Drug Delivery Rev.* **2017**, *109*, 102−118.
(3) Dekempeneer, Y.; Keyaerts, M.; Krasniqi, A.; Puttemans, J.; Muyldermans, S.; Lahoutte, T.; D'huyvetter, M.; Devoogdt, N. Targeted alpha therapy using short-lived alpha-particles and the promise of nanobodies as targeting vehicle. *Expert Opin. Biol. Ther.* **2016**, *16*, 1035−1047.
(4) Vaidyanathan, G.; Zalutsky, M. R. Applications of ^{211}At and ^{223}Ra in targeted alpha-particle radiotherapy. *Curr. Radiopharm.* **2011**, *4*, 283−294.
(5) Zalutsky, M. R.; Pruszynski, M. Astatine-211: Production and Availability. *Curr. Radiopharm.* **2011**, *4*, 177−185.
(6) Vaidyanathan, G.; Larsen, R. H.; Zalutsky, M. R. 5-[^{211}At] Astato-2'-deoxyuridine, an α-particle-emitting endoradiotherapeutic agent undergoing DNA incorporation. *Cancer Res.* **1996**, *56*, 1204−1209.
(7) Vaidyanathan, G.; Zalutsky, M. R. 1-(m-[^{211}At]astatobenzyl)-guanidine: synthesis via astato demetalation and preliminary in vitro and in vivo evaluation. *Bioconjugate Chem.* **1992**, *3*, 499−503.
(8) Foulon, C. F.; Alston, K. L.; Zalutsky, M. R. Astatin-211-labeled biotin conjugates resistant to biotinidase for use in pretargeted radioimmunotherapy. *Nucl. Med. Biol.* **1998**, *25*, 81−88.
(9) Meyer, G. J.; Walte, A.; Sriyapureddy, S. R.; Grote, M.; Krull, D.; Korkmaz, Z.; Knapp, W. H. Synthesis and analysis of 2-[211At]-L-phenylalanine and 4-[211At]-L-phenylalanine and their uptake in human glioma cell cultures in-vitro. *Appl. Radiat. Isot.* **2010**, *68*, 1060−1065.
(10) Murud, K. M.; Larsen, R. H.; Bruland, Ø. S.; Hoff, P. Influence of pretreatment with 3-amino-1-hydroxypropylidene-1,1-bisphosphonate (APB) on organ uptake of ^{211}At and ^{125}I-labeled amidobisphosphonates in mice. *Nucl. Med. Biol.* **1999**, *26*, 791−794.
(11) Zalutsky, M. R.; Reardon, D. A.; Akabani, G.; Coleman, R. E.; Friedman, A. H.; Friedman, H. S.; McLendon, R. E.; Wong, T. Z.; Bigner, D. D. Clinical experience with α-particle-emitting ^{211}At: Treatment of recurrent brain tumor patients with ^{211}At-labeled chimeric antitenascin monoclonal antibody 81C6. *J. Nucl. Med.* **2008**, *49*, 30−38.
(12) Andersson, H.; Cederkrantz, E.; Bäck, T.; Divgi, C.; Elgqvist, J.; Himmelman, J.; Horvath, G.; Jacobsson, L.; Jensen, H.; Lindegren, S.; Palm, S.; Hultborn, R. Intraperitoneal α-particle radioimmunotherapy of ovarian cancer patients: Pharmacokinetics and dosimetry of ^{211}At-MX35 F(ab')$_2$- a phase I study. *J. Nucl. Med.* **2009**, *50*, 1153−1160.
(13) Wilbur, D. S.; Thakar, M. S.; Hamlin, D. K.; Santos, E. B.; Chyan, M.-K.; Nakamae, H.; Pagel, J. M.; Press, O. W.; Sandmaier, B. M. Reagents for astatination of biomolecules. 4. Comparision of maleimido-closo-decaborate(2-) and meta-[^{211}At]astatobenzoate conjugates for labeling anti-CD45 antibodies with [^{211}At]astatine. *Bioconjugate Chem.* **2009**, *20*, 1983−1991.
(14) Green, D. J.; Shadman, M.; Jones, J. C.; Frayo, S. L.; Kenoyer, A. L.; Hylarides, M. D.; Hamlin, D. K.; Wilbur, D. S.; Balkan, E. R.; Lin, Y.; Miller, B. W.; Frost, S. H. L.; Gopal, A. K.; Orozco, J. J.; Gooley, T. A.; Laird, K. L.; Till, B. G.; Bäck, T.; Sandmaier, B. M.; Pagel, J. M.; Press, O. W. Astatine-211 conjugated to an anti-CD20 monoclonal antibody eradicates disseminated B-cell lymphoma in a mouse model. *Blood* **2015**, *125*, 2111−2119.
(15) Lindegren, S.; Andrade, L. N. S.; Bäck, T.; Machado, C. M. L.; Horta, B. B.; Buchpiguel, C.; Moro, A. M.; Okamoto, O. K.; Jacobsson,

L.; Cederkrantz, E.; Washiyama, K.; Aneheim, E.; Palm, S.; Jensen, H.; Tuma, M. C. B.; Chammas, R.; Hultborn, R.; Albertsson, P. Binding affinity, specificity and comparative biodistribution of the parental murine monoclonal antibody MX35 (anti-NaPi2b) and its humanized version Rebmab 200. *PLoS One* **2015**, *10*, No. e0126298.

(16) Li, H. K.; Morokoshi, Y.; Nagatsu, K.; Kamada, T.; Hasegawa, S. Locoregional therapy with α-emitting trastuzumab against peritoneal metastasis of human epidermal growth factor receptor 2-positive gastric cancer in mice. *Cancer Sci.* **2017**, *108*, 1648−1656.

(17) Li, H. K.; Hasegawa, S.; Nakajima, N. I.; Morokoshi, Y.; Minegishi, K.; Nagatsu, K. Targeted cancer cell ablation in mice by an α-particle-emitting astatine-211-labeled antibody against major histocompatibility complex class I chain-related protein A and B. *Biochem. Biophys. Res. Commun.* **2018**, *506*, 1078−1084.

(18) Dekempeneer, Y.; Bäck, T.; Aneheim, E.; Jensen, H.; Puttemans, J.; Xavier, C.; Keyaerts, M.; Palm, S.; Albertsson, P.; Lahoutte, T.; Caveliers, V.; Lindegren, S.; D'Huyvetter, M. Labeling of anti-HER2 nanobodies with astatine-211: Optimization and the effect of different coupling reagents on their in vivo behavior. *Mol. Pharm.* **2019**, *16*, 3524−3533.

(19) Li, Y.; Hamlin, D. K.; Chyan, M.-K.; Wong, R.; Dorman, E. F.; Emery, R. C.; Woodle, D. R.; Manger, R. L.; Nartea, M.; Kenoyer, A. L.; Orozco, J. J.; Green, D. J.; Press, O. W.; Storb, R.; Sandmaier, B. M.; Wilbur, D. S. cGMP production of astatine-211-labeled anti-CD45 antibodies for use in allogeneic hematopoietic cell transplantation for treatment of advanced hematopoietic malignancies. *PLoS One* **2018**, *13*, No. e0205135.

(20) Garrison, W. M. Reaction mechanims in the radiolysis of peptides, polypeptides, and proteins. *Chem. Rev.* **1987**, *87*, 381−398.

(21) Chakrabarti, M. C.; Le, N.; Paik, C. H.; De Graff, W. G.; Carrasquillo, J. A. Prevention of radiolysis of monoclonal antibody during labeling. *J. Nucl. Med.* **1996**, *37*, 1384−1388.

(22) Kukis, D. L.; DeNardo, S. J.; DeNardo, G. L.; O'Donnell, R. T.; Meares, C. F. Optimized conditions for chelation of Yttrium-90-DOTA immunoconjugates. *J. Nucl. Med.* **1998**, *39*, 2105−2110.

(23) McDevitt, M. R.; Fin, R. D.; Ma, D.; Larson, S. M.; Scheinberg, D. A. Preparation of alpha-emitting ^{213}Bi-labeled antibody construscts foe clinical use. *J. Nucl. Med.* **1999**, *40*, 1722−1727.

(24) Liu, S.; Edwards, D. S. Stabilization of 90Y-labeled DOTA-biomolecule conjugates using gentisic acid and ascorbic acid. *Bioconjugate Chem.* **2001**, *12*, 554−558.

(25) Lindegren, S.; Frost, S.; Bäck, T.; Haglund, E.; Elgqvist, J.; Jensen, H. Direct procedure for the production of ^{211}At-labeled antibodies with an ε-lysyl-3-(trimethylstannyl)benzamide immunoconjugate. *J. Nucl. Med.* **2008**, *49*, 1537−1545.

(26) Aneheim, E.; Gustafsson, A.; Albertsson, P.; Bäck, T.; Jensen, H.; Palm, S.; Svedhem, S.; Lindegren, S. Synthesis and evaluation of astatinated N-[2-(maleimido)ethyl]-3-(trimethylstannyl)benzamide immunoconjugates. *Bioconjugate Chem.* **2016**, *27*, 688−697.

(27) Takashima, H.; Koga, Y.; Manabe, S.; Ohnuki, K.; Tsumura, R.; Anzai, T.; Iwata, N.; Wang, Y.; Yokokita, T.; Komori, Y.; Mori, D.; Usuda, S.; Haba, H.; Fujii, H.; Matsumura, Y.; Yasunaga, M. Antitumor effect of an ^{211}At-labeled anti-tissue factor antibody protected by sodium ascorbate in gastric cancer xenograft models. *Cancer Sci* **2021**, *112*, 1975.

(28) Zhu, H.; Jia, Z.; Trush, M.; Li, Y. R. A highly sensitive chemiluminometric assay for real-time detection of biological hydrogen peroxide formation. *React. Oxygen Species* **2016**, *1*, 216−227.

(29) Safety Data Sheet in Globally Harmonized System of Classification and Labelling of Chemicals for sodium ascorbate and L-cysteine.

https://doi.org/10.1021/acsomega.1c00684
ACS Omega 2021, 6, 14887−14895